Journal of Applied Polymer Science

Molecularly Imprinted Electrochemical Sensor for the Determination of Ampicillin Based on a Gold Nanoparticle and Multiwalled Carbon Nanotube-Coated Pt Electrode

Shoulian Wei, Yong Liu, Tao Hua, Ling Liu, Hongwu Wang
Faculty of Chemistry and Chemical Engineering, Zhaoqing University, Zhaoqing 526061, People's Republic of China
Correspondence to: S. Wei (E-mail: weishlmary@126.com) or H. Wang (E-mail: hwwang@zqu.edu.cn)

ABSTRACT: A novel molecularly imprinted electrochemical sensor was developed for the sensitive and selective determination of ampicillin (AMP). The sensor was prepared on a platinum electrode modified with multiwalled carbon nanotubes (MWCNTs), gold nanoparticles (AuNPs), and a thin film of molecularly imprinted polymers (MIPs). MWCNTs and AuNPs were introduced to enhance the sensor's electronic transmission and sensitivity. The molecularly imprinted polymer (MIP) was synthesized using AMP as the template molecule, methacrylic acid as functional monomer, and ethylene glycol maleic rosinate acrylate (EGMRA) as cross-linker. The performance of the proposed imprinted sensor was investigated using cyclic voltammetry (CV), differential pulse voltammetry (DPV), and electrochemical impedance spectroscopy (EIS). The results showed that the imprinted film displayed a fast and sensitive response to AMP. Under optimal conditions, response peak current had a linear relationship with the concentration of AMP in the range of 1.0×10^{-8} mol/L to 5.0×10^{-6} mol/L and a detection limit of 1.0×10^{-9} mol/L ($S/N = 3$). This imprinted sensor was used to detect AMP in food samples with recoveries of 91.4–105%. © 2014 Wiley Periodicals, Inc. J. Appl. Polym. Sci. **2014**, *131*, 40613.

KEYWORDS: electrochemistry; sensors and actuators; nanostructured polymers

Received 26 November 2013; accepted 18 February 2014
DOI: 10.1002/app.40613

INTRODUCTION

Ampicillin sodium (AMP-Na), which belongs to a type of penicillin antibiotic medicines, is frequently used in livestock production for treating bacterial infection and as a prophylactic drug to augment growth and yield.[1–3] The extensive use of antibiotics in agriculture may lead to trace residues in food supplies, such as milk and eggs, causing a human health hazard. To protect the public health, the maximum residue limits (MRLs) for ampicillin (AMP) residues in different food commodities set by the European Union is 4 μg/kg.[4] Thus, a fast, sensitive and accurate method for the determination of AMP in food is desirable.

Many methods have been developed for detection of AMP, such as bioassays,[5,6] a UV-spectrophotometric method,[7] a fluorescence spectrophotometric method,[8] liquid-chromatography and mass-spectrometry,[9–11] capillary electrophoresis,[12] and immunological methods.[13,14] However, these methods suffer from either low selectivity and sensitivity or time-consuming analysis processes.

An electrochemical sensor is an attractive method for determination of AMP due to high sensitivity, fast response, low cost, stability, and ease of operation. Molecularly imprinted polymers (MIPs) as sensing materials possess tailor-made affinity and selectivity for the target molecule.[15,16] MIPs are usually synthesized by combining template molecules with functional monomers and subsequent copolymerization with cross-linking monomers. Removal of the template molecules leaves cavities (recognition sites) that are complementary in size, shape, and functional groups to the analyte. Recently, several MIPs-based sensors to detect antibiotics have been reported and the selectivity has improved.[17,18] However, the use of MIPs as sensing materials often suffers from some drawbacks, such as poor mass transfer, slow binding kinetics, and low sensitivity.[19] Thus, the proper design of signal transducer still remains a challenge to the MIPs modified electrode. Several studies demonstrated the use of imprinted thin films and nanoparticles to obtain a quick response and enhance sensitivity. Lian et al. reported a molecularly imprinted electrochemical sensor based on β-cyclodextrin incorporated multiwalled carbon nanotubes (MWCNTs), gold nanoparticles-polyamide amine dendrimer nanocomposites (Au-PAMAM), and chitosan derivative (CSDT) coated electrode for selective determination of chlortetracycline with a detection limit of 4.954×10^{-8} mol/L.[20] Zhang et al. demonstrated that a layer-by-layer assembly molecularly imprinted sol-gel sensor based on MWCNTs coated electrode for selective recognition of

clindamycin with a detection limit of 2.44×10^{-8} mol/L.[21] Hu et al. developed an imprinted sol–gel electrochemical sensor based on MWCNTs doped with a chitosan film for the determination of benzylpenicillin with a detection limit of 1.5×10^{-9} mol/L, which effectively enhanced signal intensity.[22] Huang et al. also developed an electrochemical sensor to detect bisphenol A based on imprinted sol–gel and MWCNTs and gold nanoparticles (AuNPs) with a detection limit of 3.6×10^{-9} mol/L.[23] However, as far as we know, there are no reports on the detection of AMP by molecularly imprinted sensors.

The aim of this work was to construct an electrochemical sensor for the detection of AMP using a molecular imprinting technique. MWCNTs and AuNPs were introduced during the preparation of an imprinted sensor to enhance the current response sensitivity of the sensor. The sensor was prepared on a platinum electrode modified with MWCNTs, AuNPs, and a thin film of MIPs, and the MIPs were synthesized using ampicillin as a template molecule, methacrylic acid as a functional monomer, and ethylene glycol maleic rosinate acrylate (EGMRA) as a cross-linker. The MIPs have the thin yet rigid medium, good stability, rapid response, and high selectivity for the determination of AMP in food samples.

EXPERIMENTAL

Reagents

MWCNTs with diameters of 50 nm were purchased from the Shenzhen Nanotubes Company Ltd (China). KCl, N,N-dimethylformamide (DMF), methanol, and ethanol were purchased from Guangzhou Reagent Factory (China). EGMRA was gifted by the College of Chemistry and Ecological Engineering, Guangxi University for Nationalities (China). AIBN, MAA, and chloroauric acid were purchased from Aladdin Chemistry Co., Ltd. (China). AMP was obtained from Xi'an Pharmaceutical Co. (China). Other chemicals were analytical reagent grade. Double-distilled water was used in all experiments.

Equipment

Electrochemical experiments were carried out on a CHI660B electrochemical workstation (Shanghai Chenhua Apparatus Co.). Electrochemical measurements were performed with a three-electrode system composed of a platinum wire as auxiliary electrode, an Ag/AgCl electrode as reference electrode and a modified platinum electrode as the working electrode. pH was measured using a PHS-3C pH meter (Dapu Instrumentation Corp, Ltd. Shanghai, China).

Preparation of MIP and Non-Molecularly Imprinted Polymer (NIP)

To prepare the MIP for AMP, 0.5 mmol of MAA and 0.1 mmol AMP-Na were mixed in 3.0 mL absolute alcohol, and the mixture was sonicated for 15 min. Then, 0.4 mmol of EGMRA and 0.01 g AIBN were added, and the mixture was sonicated for 15 min until a homogeneous solution was obtained. Finally, the AMP-imprinted polymer solution was obtained by bubbling nitrogen for 5 min to remove dissolved oxygen.

As a control, the NIP solution was prepared in the same way mentioned above but without the addition of AMP-Na.

Preparation of AuNPs and MWCNTs

AuNPs were prepared by using a previously reported procedure.[24] 0.010 g $HAuCl_4$ was dissolved into 100 mL of double-distilled water and boiled. A 2.0 mL of a 1% trisodium citrate solution for the preparation of AuNPs was quickly added to the refluxed $HAuCl_4$ solution, resulting in a rapid color change from pale yellow to deep red that indicated the formation of AuNPs. The AuNPs solution was stored at 4°C when not in use.

MWCNTs were prepared with the method described in reference.[25] A mixture of 50 mg MWCNTs was added to 50 mL of HNO_3 under sonication for 10 min. Then, the mixture was stirred under 85°C for 12 h. After cooling to room temperature, the mixture was filtered through a 0.22 μm polycarbonate membrane and washed thoroughly with redistilled water several times until filtrate pH was neutral. The filtered solid was dried under vacuum for 12 h, producing carboxylic acid-functionalized MWCNTs (MWCNTs–COOH). A mixture of 5.0 mg functionalized MWCNTs was dispersed in 5.0 mL DMF and 5.0 mL redistilled water by ultrasonic agitation for 20 min to give a homogeneous MWCNT suspension.

Preparation of Imprinted Sensor

Prior to use, a platinum electrode was polished carefully with a 0.05 μm alumina slurry to a mirror finish, rinsed, and sonicated in double-distilled water and ethanol for 5 min. Then it was subjected cyclical sweeps between +0.8 V and −0.2 V in a 5.0 mmol/L solution of $K_3[Fe(CN)_6]$ containing 0.2 mol/L KCl until a stable cyclic voltammogram (CV) was obtained. Finally, it was rinsed with double-distilled water and dried.

Preparation of the AMP-imprinted sensor (Figure 1): First, 4 μL of the AuNPs solution was dropped onto the platinum electrode and the electrode was dried at 60°C for 4 h. Then, 4 μL of the functionalized MWCNTs suspension was added on the AuNPs modified electrode and dried at 60°C for 4 h. Finally, 4 μL of the prepared MIPs solution of AMP was coated on the AuNPs/MWCNTs modified electrode and dried at 60°C for 6 h. Thus, an AMP-imprinted sensor was successfully fabricated. The template molecule was removed from the imprinted film by immersion in a solution of methanol containing 10% acetic acid for 5 min.

The drying temperature was kept in 60°C, while the temperature was over 60°C which would cause some disadvantages: (1) the membranes formed were rough and easy to crack; (2) the carbon nanotubes with small diameter and high surface energy were very easy to agglomerate, which affect binding polymer interface and electronic conductivity; (3) the gold nanoparticles were easy to gather, which reduced the electronic conductivity.

The NIPs sensor was prepared following the same experimental procedures except omitting the addition of AMP.

Electrochemical Measurement

Electrochemical measurements were carried out in a 10 mL aqueous solution containing 5.0 mmol/L of $K_3[Fe(CN)_6]$ and 0.2 mol/L of KCl at room temperature. CV measurements were taken from −0.2 V to +0.8 V at a scan rate of 100 mV/s. Differential pulse voltammetry (DPV) was performed from +0.6 V to −0.2 V, the pulse amplitude was 50 mV, the pulse width was

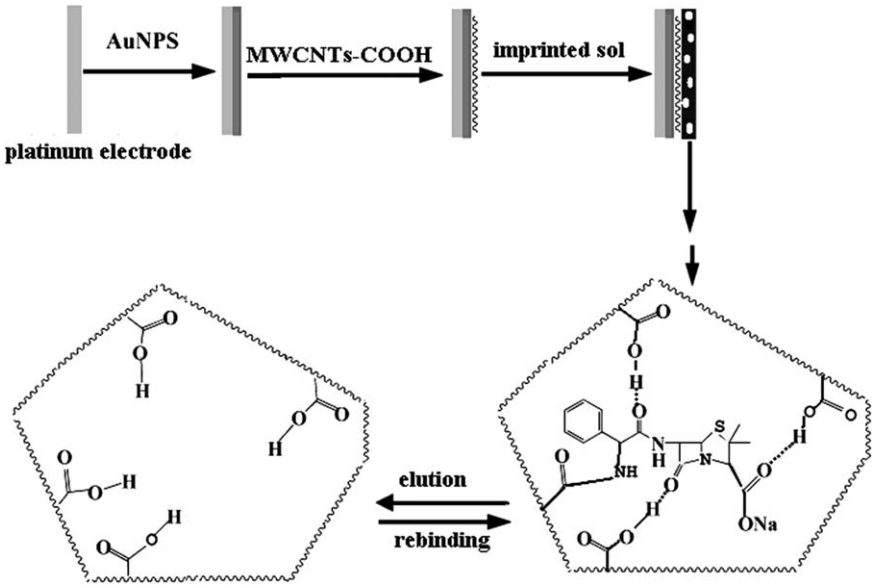

Figure 1. Schematic representation for the preparation of MIP/MWCNTs/AuNPs/Pt electrode.

0.2 s, and the pulse period was 0.5 s. Electrochemical impedance spectroscopy (EIS) measurements were carried out in a frequency range from 0.1 Hz to 10^5 Hz. The amplitude of the alternating voltage was 5.0 mV.

Sample Preparation

Milk, a feed sample, and fresh eggs were purchased from local markets and stored at 4°C until analysis.

A 5 mL milk sample was placed in a 20 mL polypropylene centrifuge tube and 10 mL of acetonitrile was added to promote protein precipitation. The mixture was vortexed for 1 min, sat for 10 min, and centrifuged for 20 min at 4000 rpm. Then, the supernatant was collected and evaporated to dry under a gentle stream of nitrogen at 50°C in a water bath. The obtained residues were redissolved in 2 mL of redistilled water.

The feed sample was pulverized using a domestic grinder to obtain a homogeneous powder, and 5 g was weighed into a 120 mL polypropylene centrifuge tube and 100 mL of water/acetonitrile solution (75 : 25, v/v) was added. The mixture was vortexed for 2 min, sonicated for 30 min, and centrifuged for 15 min at 4000 rpm. The supernatant was collected and evaporated to dry under a gentle stream of nitrogen at 50°C in a water bath. The obtained residues were redissolved in 2 mL of redistilled water.

A whole egg was homogenized for 10 min using a magnetic stirrer, and 5 g was transferred into a 50 mL polypropylene centrifuge tube and 25 mL of acetonitrile was added. The mixture was vortexed for 2 min, sonicated for 30 min, and centrifuged for 15 min at 4000 rpm. The supernatant was collected and evaporated to dry under a gentle stream of nitrogen at 50°C in a water bath. The obtained residues were redissolved in 2 mL of redistilled water.

RESULTS AND DISCUSSION

Characterization of the MIP Modified Electrode

Cyclic voltammograms (CV) of the different modified electrodes in aqueous solutions containing 5.0 mmol/L of $K_3[Fe(CN)_6]$ and 0.2 mol/L of KCl as the indicator substance are shown in Figure 2. Figure 2 shows that the CV of $K_3[Fe(CN)_6]$ in aqueous solution of KCl for a bare platinum electrode gives a pair of redox peaks. After the surface was covered with a layer AuNPs or MWCNTs, current of redox peaks increased, obviously owing to the AuNPs or MWCNTs, which increase surface area and active sites for electron transfer [Figure 2(b,c)]. Coupled with the introduction of the AuNPs and MWCNTs, current of redox peaks further increased [Figure 2(d)], which suggested that AuNPs and MWCNTs were firmly adhered to the electrode surface, and effectively increased surface area and active sites of the electrode. However, when the MIP film was coated on the surface of MWCNTs/AuNPs–Pt electrode, the redox peak current disappeared [Figure 2(f)]. The reason was that the molecules of $K_3[Fe(CN)_6]$ could not penetrate through the polymer layer and arrive at the surface of electrode. After the template was

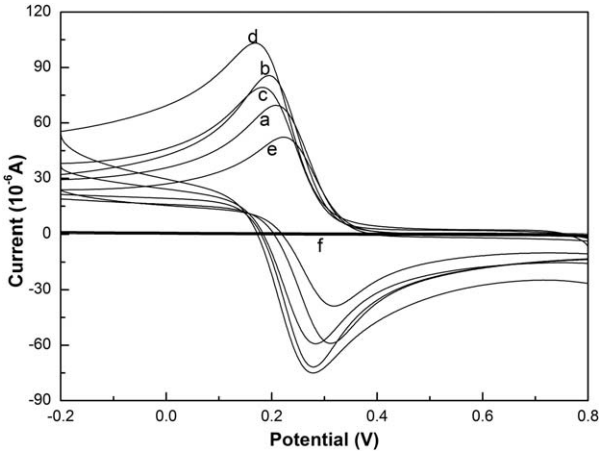

Figure 2. Cyclic voltammograms of bare Pt (a); AuNPs/Pt (b); MWCNTs/Pt (c); MWCNTs/AuNPs/Pt (d); MIP/MWCNTs/AuNPs/Pt after removal of AMP (e); MIP/MWCNTs/AuNPs/Pt before removal of AMP (f) in 5 mmol/L of K3[Fe(CN)6] and 0.2 mol/L of KCl solution (pH 6.0).

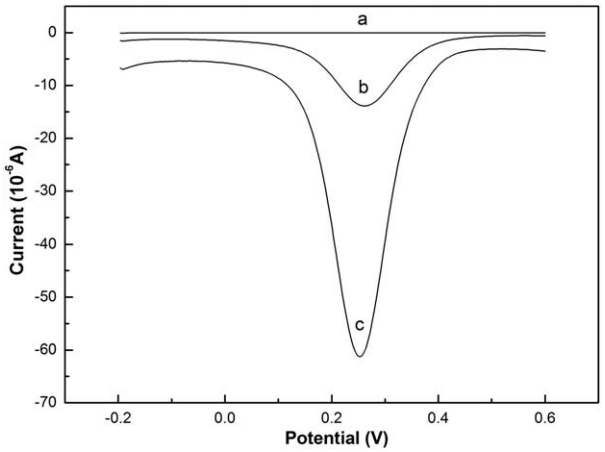

Figure 3. DPV curves of the MIP/MWCNTs/AuNPs/Pt before extraction of AMP (a); after incubated in 1.0×10^{-5} M AMP solution for 5 min (b); after extraction of AMP (c); Supporting electrolyte: 5 mmol/L of $K_3[Fe(CN)_6]$ and 0.2 mol/L of KCl solution (pH 6.0).

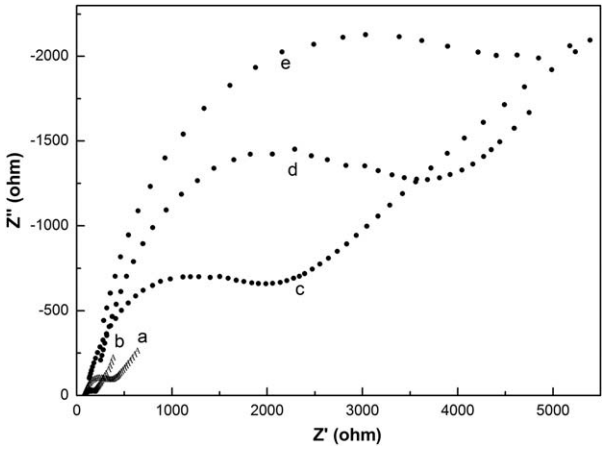

Figure 4. the electrochemical impedance spectra of bare Pt (a); MWCNTs/AuNPs/Pt (b); MIP/MWCNTs/AuNPs/Pt after (c) and before removal of AMP (d); NIP/MWCNTs/AuNPs/Pt (e) in 5 mmol/L of $K_3[Fe(CN)_6]$ and 0.2 mol/L of KCl solution (pH 6.0).

removed from the MIP sensor, the redox current peaks returned [Figure 2(e)]. This is due to the formation of vacant recognition sites or binding cavities after removing the template, which made electronic transmission possible since $K_3[Fe(CN)_6]$ could easily pass through the cavity and reach the surface of the electrode.

DPV was also used to characterize the imprinted sensor. Figure 3 shows the typical DPV responses of the imprimted electrode in different conditions. No peaks were observed at 0.25 V (curve a) for an imprinted electrode before extraction of AMP due to non-conductance of the template molecules and insulativity of the MIP film. However, when the imprinted electrode was eluted with a methanol-acetic acid solution (1 : 1, v : v) for 5 min, a significant and typical reductive peak was obtained at 0.25 V (curve c), confirming that AMP template molecules were removed effectively. When the imprinted electrode was incubated in a 1.0×10^{-5} mol/L AMP solution for 5 min, the reductive peak diminished sharply (curve b), exhibiting the excellent affinity and rebinding ability of the MIP/MWCNTs/AuNPs/Pt electrochemical sensor to AMP molecules.

Electrochemical impedance spectroscopy (EIS) is an efficient tool for studying the features of surface-modified electrodes. Figure 4 shows the electrochemical impedance spectra of a bare Pt electrode, a MWCNTs/AuNPs/Pt electrode, a MIP/MWCNTs/AuNPs/Pt electrode before and after removal of AMP, NIP/MWCNTs/AuNPs/Pt electrode, respectively. In EIS, the semicircle diameter equals the electron transfer resistance (R_{et}), which controls the electron-transfer kinetics of the redox probe at the electrode interface.[26] As shown in Figure 4, the R_{et} of the bare electrode (curve a) was larger than that of the MWCNTs/AuNPs/Pt (curve b), showing that MWCNTs and AuNPs promoted electron transfer of the electrochemical probe. After the polymer film was coated to the surface of a MWCNTs/AuNPs/Pt electrode, the R_{et} increased (curves c and d), indicating that the polymer film blocked the interfacial electron transfer. It is worth noting that R_{et} of the NIP film (curve e) is larger than that of the MIP film (d), and after removal of AMP molecules, a further decrease of resistance was observed for the MIPs modified electrode (curve c). The reason was that more imprinted cavities were formed on the MIP film after removal of templates, which served as an electron transfer pathway for the electrochemical probe. These results are in agreement with the CV curves as described in details above.

Optimization of the Experimental Conditions

Effect of the Amount of MAA and EGMRA on the Response of the Sensor. The effects of the amount of MAA and EGMRA on the CV responses of the MIP/MWCNTs/AuNPs/Pt electrode were studied by fixing the amount of template molecular AMP at 0.1 mmol. As shown in Figure 5, when the amount of MAA was 0.4 mmol, the current response was small. The reason was that the number of functional monomer was not enough to combine with template molecules, generating rather few special binding sites to respond to relatively low current. The largest current response was found when using an amount of 0.5 mmol for MAA. When the amount of MAA exceeded 0.5 mmol, the current response decreased. The reason may be that

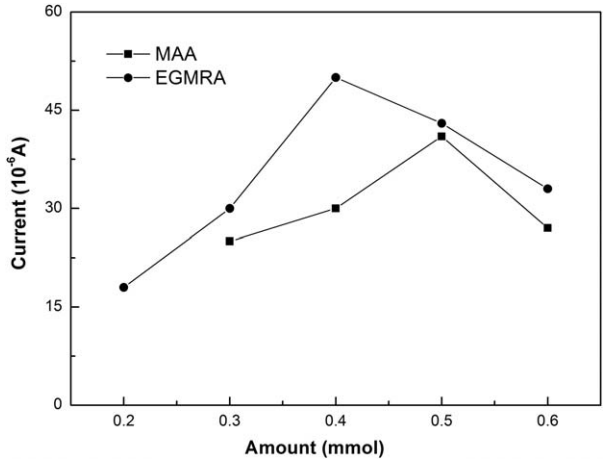

Figure 5. Effect of the amount of MAA and EGMRA in the presence of 0.1 mmol AMP.

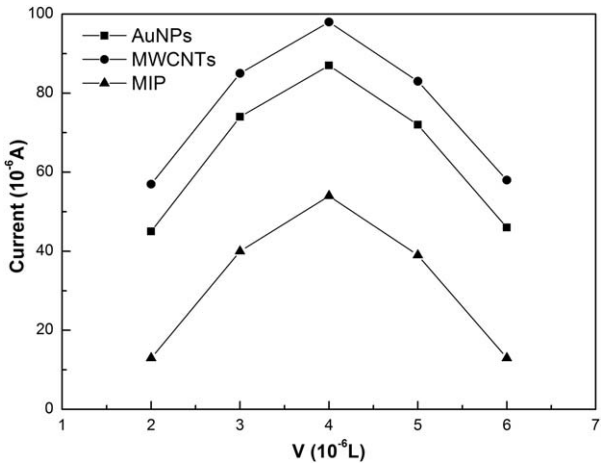

Figure 6. Effect of the volume of the composite.

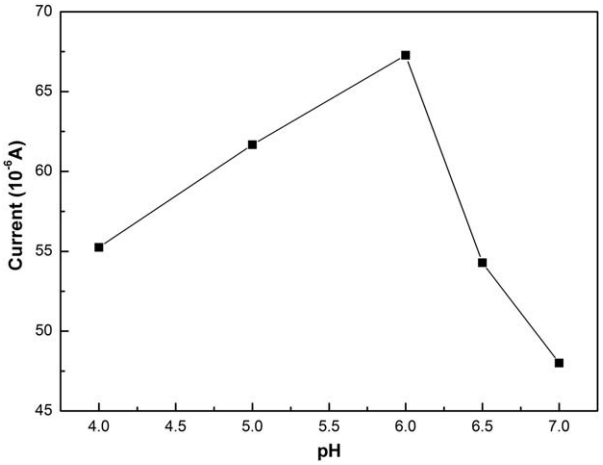

Figure 7. Effect of pH of the supporting electrolyte solution.

the special binding sites of MIP declined with the increase of monomer, which generated heterogeneity in binding sites.[27]

The effect of the cross-linker, EGMRA, amount in the presence of 0.5 mmol MAA and 0.1 mmol AMP was shown in Figure 5. With the amount of EGMRA increasing, the current responses increased quickly at first and then decreased gradually. The largest current response was observed when using an amount of 0.4 mmol EGMRA. The reason was that imprinted cavities were stabilized without any deformation after the removal of templates. However, when the EGMRA amount exceeded 0.4 mmol, the structure of the film may have become stiffer and denser, significantly restricting access to the cavities and resulting in lower current. Thus, the mole ratio of 1 : 5 : 4 for template: monomer: cross-linker was chosen as the optimum.

Effect of the Volume of the Composite. Effect of the volume of the composite (AuNPs, MWCNTs, and MIP) on the current response was investigated in the range of 2–6 μL. As shown in Figure 6, the current response increased with increasing the volume of composite from 2 to 4 μL, and then it decreased. This is because when the volume of the composite is less than 4 μL, the modified film cannot cover the surface of the electrode, hence there is not enough the surface area of the electrode or effective imprinted sites to produce an operable sensor. However, when the volume of the composite is more than 4 μL, the modified film is too thick for electron transfer, leading to a lower current response. Therefore, 4 μL was chosen as the best volume.

Influence of pH. The effect of pH of the supporting electrolyte solution on the DPV response of AMP was tested. As shown in Figure 7, as the supporting electrolyte solution pH increased from 4 to 6, the current response increased. When the solution pH was over 6.0, the current response decreased owing to the interference of OH^-. The maximum current response was obtained at pH 6.0.

The effect of pH of the AMP sample solution on the AMP extraction in the electrode was studied also. The results in Figure 8 show that the current response significantly increased with increased pH from 4 to 6, and then decreased with further increased pH. It can be attributed to the competitive binding of H^+ with –COOH of the AMP-imprinted polymer for AMP at a low pH. Beyond pH 6, the competitive binding of OH^- with AMP for –COOH of the AMP- imprinted polymer. Thus, the optimum pH of the AMP sample solution on the AMP extraction was 6.0.

Influence of Scan Rate. To study the predominant type of mass transport, CVs of the MIP sensor in a 5.0 mmol/L of $K_3[Fe(CN)_6]$ containing 0.2 mol/L of KCl solution (pH 6.0) at different scan rates were investigated. As shown in Figure 9, with increasing the scan rate from 20 to 100 mV/s, both the cathodic and anodic peak currents increased and their potentials show considerable shift. The reason may be imprinted polymer membrane has a slight adsorption on ferricyanide. When the scanning speed is too low, the need to increase the applied voltage to overcome the adsorption effect, so the reduction peak potential of ferricyanide shifted negatively and the oxidation peak potential shifted positively, the peak potential difference is relatively large. With the increase of scanning speed, the applied voltage increases, the adsorption of ferricyanide is overcome, the redox peak potential shifted to the equilibrium potential, peak potential difference is about 56∼60 mV, electron transfer

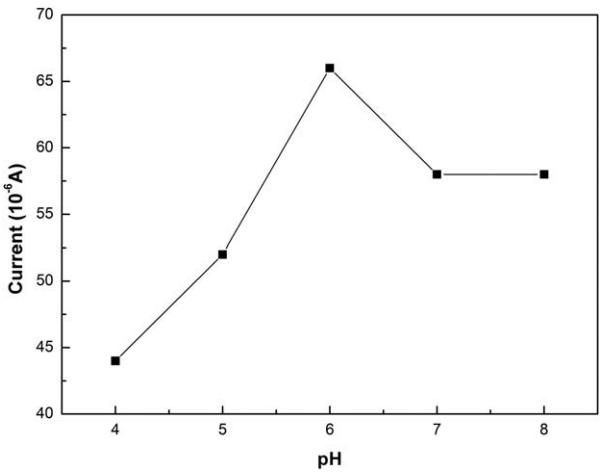

Figure 8. Effect of pH of the AMP sample solution on the AMP extraction in the electrode.

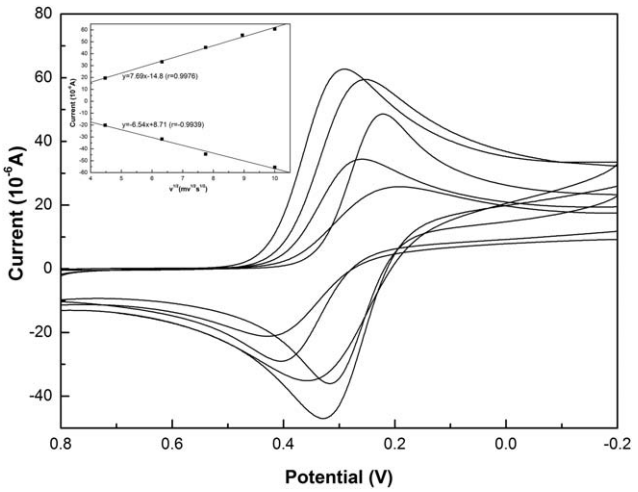

Figure 9. Cyclic voltammograms of the MIP/MWCNTs/AuNPs/Pt in a 5 mmol/L $K_3Fe(CN)_6$ containing 0.2 mol/L KCl solution at different scan rate.

reaction of ferricyanide is reversible. In addition, the cathodic and anodic peak current and the square root of scan rate showed a linear relationship, indicating that the electrode process is diffusion-controlled.[28]

Influence of Incubation Time. Incubation time affects the sensitivity of the response of the MIP sensor to its template. The MIP sensor after removal the template was incubated in a 1.0 $\times$ 10^{-5} mol/L AMP standard solution for different times, rinsed by doubly distilled water, dried with filter paper in turn, and then put into the supporting electrolyte solution to measure the peak current quantitatively by DPV. As shown in Figure 10, the peak current decreased rapidly with an increase of incubation time from 1 to 10 min. The reason was that partial binding sites in MIP films were occupied by AMP. After 10 min of incubation, a stable response was obtained, suggesting that the adsorption equilibrium was reached. So an incubation time of 10 min was selected for the imprinted sensor.

Analytical Performance

Calibration Curve. Under the optimal experimental conditions, the determination of AMP at different concentrations was carried out with DPV responses. The anodic peak current was

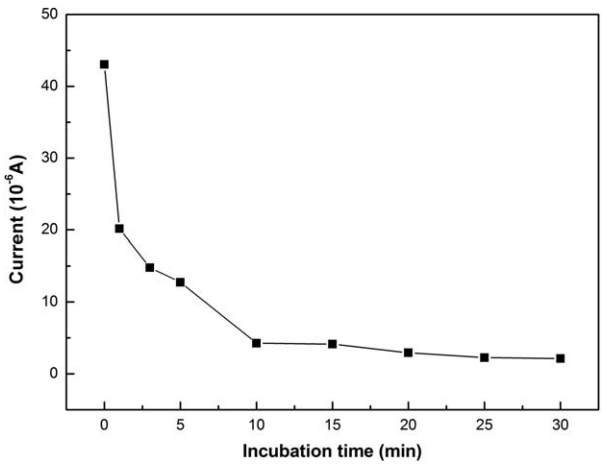

Figure 10. Effect of incubation time.

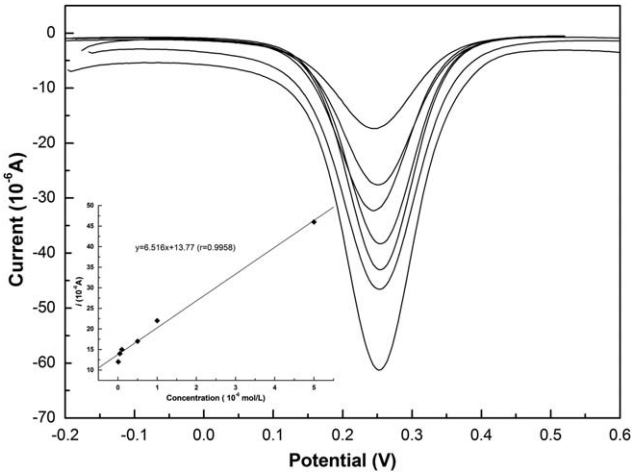

Figure 11. DPV curves of the MIP/MWCNTs/AuNPs/Pt in 5 mmol/L $K_3Fe(CN)_6$ and 0.2 mol/L KCl solution after incubation in different concentrations of AMP solution for 10 min, eluted by methanol-acetic acid solution (v : v, 5 : 5) for 5 min. The insert shows the calibration curves of AMP at the MIP/MWCNTs/AuNPs/Pt.

related linearly to the concentration of AMP from 1.0 $\times$ 10^{-8} mol/L to 5.0 $\times$ 10^{-6} mol/L (Figure 11). The linear regression equation was expressed as i (μA) = 6.517c (μmol/L) + 13.77 (R = 0.9958). The limit of detection (LOD) was estimated to be 1.0 $\times$ 10^{-9} mol/L ($S/N = 3$), which was lower than the MRL established by the EU for the studied β-lactams in foodstuffs of animal origin . It makes the method suitable for routine control analysis.

Sensor Selectivity. The selectivity of the MIP sensor for AMP was evaluated by DPV determination of AMP or AMP in the

Table I. Selectivity of the Imprinted Sensors ($n = 3$)

Samples	i/μA	Error/%	K^*
0.5 μM AMP	34.1		
0.5 μM AMP+0.5 μM Amoxicillin	32.1	−5.9	1.07
0.5 μM AMP+0.5 μM Penicillin	31.5	−7.6	1.09
0.5 μM AMP+0.5 μM Piperacllin	30.2	−11.4	1.14
1000-fold of $CaCl_2$	34.1	0	1.00
1000-fold of NaCl	34.3	0.6	0.99
1000-fold of lactic acid	33.5	−1.8	1.02
500-fold of cane sugar	33.4	−2.1	1.02
500-fold of glucose	33.0	−3.2	1.04
500-fold of starch	33.2	−2.6	1.03
500-fold of lactose	32.7	−4.1	1.05
100-fold of urea	34.4	0.9	0.99
100-fold of tyrosine	32.6	−4.4	1.05
100-fold of phenylalanine	32.8	−3.8	1.05
100-fold of Lysine	33.3	−2.3	1.03
100-fold of leucine	32.9	−3.5	1.04
100-fold of tryptophan	33.5	−1.8	1.02
100-fold of methionine	33.6	−1.5	1.02

presence of some analogues and common materials including amoxicillin, penicillin, piperacillin, cane sugar, glucose, starch, lactose, urea, $CaCl_2$, NaCl, lactic acid, tyrosine, phenylalanine, lysine, leucine, tryptophan, and methionine in food samples. As shown in Table I, the MIP sensor yielded almost the same response for 0.5 μmol/L AMP and the mixture of 0.5 μmol/L AMP, and the structural analogs within the same concentration level. In addition, the selectivity coefficients, K, ($K = \Delta i_{int}/\Delta i_{amp}$) were also used to evaluate the analogues by using method known method.[29] The selectivity coefficients of amoxicillin, penicillin, and piperacillin were 1.07, 1.09, and 1.14, respectively, indicating the imprinted sensor has good selectivity for AMP. This can be explained by the size and contours of cavities in the MIP film matching AMP. Furthermore, it was also found that the presence of 1000-fold of $CaCl_2$, NaCl, lactic acid, 500-fold of cane sugar, glucose, starch, lactose, 100-fold of urea, tyrosine, phenylalanine, Lysine, leucine, tryptophan, and methionine did not interfere with the determination of AMP (peak current response change below ± 5%). These results demonstrated that interfering species in the determination of AMP-Na are inconsequential.

Reproducibility and Stability. The reproducibility of the imprinted sensor was determined by analyzing a solution of 0.5 μmol/L AMP with five different sensors prepared independently under the same experimental condition. As shown in Table II, three measurements from the batch resulted in a relative standard deviation of 5.5%. The repeatability of one imprinted sensor was examined by testing the DPV response using five replicates of a solution of 0.5 μmol/L AMP. The RSD of currents response was 4.5%. The long-time stability of the imprinted sensor was also investigated on a 30-day period. The sensor was used to detect the same AMP concentration (0.5 μmol/L). When stored in air at 4°C in a refrigerator, the sensor retained more than 95% of the initial current response after 15 days, and decreased to 90.0% after 30 days, which demonstrated that the sensor had good stability. The reason can be attributed to the excellent stability, mechanical strength, and cross-linking ability of EGMRA, which immobilized the imprinted film with a highly stable, rigid structure on the modified electrode surface.

Sample Analysis. The established method was applied for the determination of AMP in milk, animal feed, and fresh egg samples which were prepared following the method described in Section 2.7. The results are summarized in Table III. AMP was not detected in milk and fresh egg samples; however, a mean AMP concentration of 72.6 μg/kg was found in the feed samples, which was much higher than European standards. These three samples were spiked with AMP, each at three different concentration levels. The RSDs acquired were below 6% and the recoveries for milk, feed, and fresh egg samples varied from 91.4 to 105%, indicating that this method had good accuracy and is potentially applicable for the determination AMP in commercial food samples.

Table II. Determination Results of the 0.5 μmol/L AMP Solution with Five Different Sensors ($n = 3$)

Sensors	Found/(μmol/L)	Means/(μmol/L)	RSD/%
1	0.53, 0.49, 0.50	0.50	5.5
2	0.52, 0.51, 0.46		
3	0.52, 0.55, 0.47		
4	0.45, 0.51, 0.50		
5	0.52, 0.49, 0.53		

Table III. Analytical Results of AMP in the Food Samples ($n = 3$)

sample	Detected (ng/mL, μg/kg)	Add (ng/mL)	Found (ng/mL)	Recovery %	RSD %
milk	None	10.0	10.5	105	3.9
		20.0	19.6	98.0	3.6
		40.0	37.7	94.2	4.8
feed	72.6	30.0	100.7	93.7	4.1
		60.0	127.8	92.0	3.3
		90.0	154.9	91.4	5.7
egg	None	10.0	10.3	103	3.8
		20.0	19.6	98.0	3.4
		40.0	38.2	95.5	4.5

CONCLUSIONS

A simple, sensitive, and stable imprinted sensor was fabricated for detection of AMP by stepwise modification of a MWCNTs/AuNPs nanocomposite film with a thin MIP film on a platinum electrode. The excellent performance of the imprinted sensor to AMP can be ascribed to the MWCNTs/AuNPs nanocomposite with electrochemical catalytic activities and the molecularly imprinted film with plentiful selective binding sites. The developed sensor exhibited a low limit of detection, wide linear range, high selectivity, good repeatability and stability, and it was successfully applied for detecting AMP in food samples with satisfactory results.

ACKNOWLEDGMENTS

This work is financially supported by the Science and Technology Innovation Project of Guangdong provincial education department (No.2012kjcx0104), the Science and Technology Planning Project of Guangdong province (No. 2011B020314011), and the Natural Science Foundation of Guangdong Province (No.S2011010004004; No. S2012040007710).

REFERENCES

1. Riediker, S.; Diserens, J. M.; Stadler, R. H. *J. Agric. Food Chem.* **2001**, *49*, 4171.
2. Okeke, I. N.; Lamikanra, A.; Edelmant, R. *Emerg. Infect. Dis.* **1999**, *5*, 18.
3. Gröhn, Y. T.; Wilson, D. J.; Gonzalez, R. N.; Hertl, J. A.; Schulte, H.; Bennett, G.; Schukken, Y. H. *J. Dairy Sci.* **2007**, *90*, 2260.
4. Commission, E. *Official J. Eur. Union* **2010**, *1*, 15.
5. Messer, J. W.; Leslie, J. E.; Houghtby, G. A.; Peeler, J. T.; Barnett, J. E. *J. Assoc. Official Anal. Chem.* **1982**, *65*, 1208.

6. Plakas, S. M.; Paola, A. D.; Moxey, M. *J. Assoc. Official Anal. Chem.* **1991**, *74*, 910.
7. Mahgoub, H.; Aly, F. A. *J. Pharmaceut. Biomed. Anal.* **1998**, *17*, 1273.
8. Gala, B.; Gómez-Hens, A.; Pérez-Bendito, D. *Talanta* **1997**, *44*, 1883.
9. Evaggelopoulou, E. N.; Samanidou, V. F. *Food Chem.* **2013**, *136*, 1322.
10. Capriotti, A. L.; Cavaliere, C.; Piovesana, S.; Samperi, R.; Laganà, A. *J. Chromatogr. A* **2012**, *1268*, 84.
11. Cámara, M.; Gallego-Picó, A.; Garcinuño, R. M.; Fernández-Hernando, P.; Durand-Alegría, J. S.; Sánchez, P. *J. Food Chem.* **2013**, *141*, 829.
12. Santos, S. M.; Henriques, M.; Duarte, A. C.; Esteves, V. I. *Talanta* **2007**, *71*, 731.
13. Bacigalupo, M. A.; Meroni, G.; Secundo, F.; Lelli, R. *Talanta* **2008**, *77*, 126.
14. Benito-Pena, E.; Moreno-Bondi, M. C.; Orellana, G.; Maquieira, A.; van-Amerongen, A. *J. Agric. Food Chem.* **2005**, *53*, 6635.
15. Guerreiro, J. R. L.; Freitas, V.; Sales, M. G. F. *Microchem. J.* **2011**, *97*, 173.
16. Sun, C. L.; Chang, C. T.; Lee, H. H.; Zhou, J.; Wang, J.; Sham, T. K.; Pong, W. F. *ACS Nano* **2011**, *5*, 7788.
17. Bergmann, N. M.; Peppas, N. A. *Prog. Polym. Sci.* **2008**, *33*, 271.
18. Fuchs, Y.; Soppera, O.; Haupt, K. *Anal. Chim. Acta* **2012**, *717*, 7.
19. Matsui, J.; Okada, M.; Tsuruoka, M.; Takeuchi, T. *Anal. Commun.* **1997**, *34*, 85.
20. Lian, W.; Huang, J.; Yu, J.; Zhang, X.; Lin, Q.; He, X.; Xing, X.; Liu, S. *Food Control* **2012**, *26*, 620.
21. Zhang, Z.; Hu, Y.; Zhang, H.; Yao, S. *J. Colloid Interf. Sci.* **2010**, *344*, 158.
22. Hu, Y.; Li, J.; Zhang, Z.; Zhang, H.; Luo, L.; Yao, S. *Anal. Chim. Acta* **2011**, *698*, 61.
23. Huang, J.; Zhang, X.; Lin, Q.; He, X.; Xing, X.; Huai, H.; Lian, W.; Zhu, H. *Food Control* **2011**, *22*, 786.
24. Zhang, Y. Z.; Zhang, K. Y.; Ma, H. Y. *Am. J. Biomed. Sci.* **2009**, *1*, 115.
25. Zhang, Z.; Hu, Y.; Zhang, H.; Luo, L.; Yao, S. *Biosens. Bioelectron.* **2010**, *26*, 696.
26. Katz, E.; Willner, I. *Electroanal.* **2003**, *15*, 913.
27. Gao, X. Handbook on the physics and chemistry of rare earths; Elsevier, North-Holland, **1986**, pp 163.
28. Huang, K. J.; Niu, D. J.; Xie, W. Z.; Wang, W. *Anal. Chim. Acta* **2010**, *659*, 102.
29. Yan, X.; Deng, J.; Xu, J.; Li, H.; Wang, L.; Chen, D.; Xie, J. *Sensor. Actuat. B* **2012**, *171*, 1087.